Supplementary Information

Original Article

Tat-functionalized Ag-Fe_3O_4 nano-composites as tissue-penetrating vehicles for tumor magnetic targeting and drug delivery

Ergang Liu[a,b,c], Meng Zhang[c], Hui Cui[b], Junbo Gong[a], Yongzhuo Huang[c], Jianxin Wang[d], Yanna Cui[c], Weibing Dong[a], Lu Sun[b], Huining He[b,*], Victor C. Yang[a,b,e,*]

[a]*State Key Laboratory of Chemical Engineering, School of Chemical Engineering and Technology, Tianjin University, Tianjin 300072, China*

[b]*Tianjin Key Laboratory on Technologies Enabling Development of Clinical Therapeutics and Diagnosis, School of Pharmacy, Tianjin Medical University, Tianjin 300070, China*

[c]*Shanghai Institute of Materia Medica, Chinese Academy of Sciences, Shanghai 201203, Chin*a

[d]*Department of Pharmaceutics, School of Pharmacy, Fudan University & Key Laboratory of Smart Drug Delivery, Ministry of Education, Shanghai 201203, China*

[e]*Department of Pharmaceutical Sciences, College of Pharmacy, University of Michigan, Ann Arbor, MI 48109-1065, USA*

Received 10 March 2018; received in revised form 19 April 2018; accepted 26 June 2018

[*]Corresponding Authors. Tel./fax: +86 22 83336658.

E-mail addresses: hehuining@tmu.edu.cn (Huining He), vcyang@med.umich.edu (Victor C. Yang).

The supplemented materials provided the purification method, pH dependent drug release behavior, and cytotoxicity of metallic nanoparticles which helped to characterize the as-prepared nanovehicles. Moreover, optic images of excised organs from tumor-targeting experiment, as well as the fluorescent images of brain sections from brain-targeting experiment were also provided to explicit the targeting potential of the dual functional delivery system.

1. Purification of dextrin immobilized FeAgNPs

The freshly prepared FeAgNPs were dispersed in water. For purification, 4–5-fold of ethanol in volume was mixed with FeAgNP solution, then the mixture was left to stand for overnight, till the all of the nanocomponents had deposited at the bottom of the vials. The sediments were then washed with ethanol, and re-dispersed with predetermined volume of water to produce concentrated FeAgNPs.

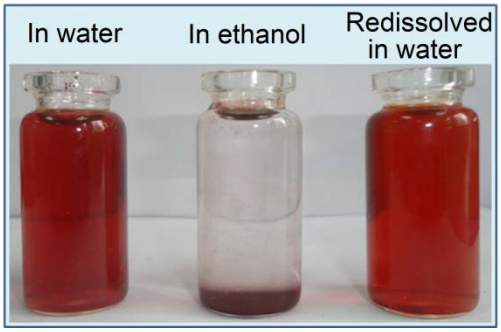

Figure S1 Solubility of dextrin immobilized Ag-Fe_3O_4 in water and ethanol, respectively.

2. Drug loading and release assays

To assess the drug loading potential of the nanoparticles, 50 mg dextrin-coated AgNPs (containing about 1.8 mg silver nanoparticles) were added into 1 mL Dox–SH solution of different concentrations (ranging 25–250 μg/mL). After incubation for 2 h, drug-loaded nanoparticles were precipitated by 8-fold excess of alcohol, centrifuged and Dox–SH content in the supernatant was quantified to calculate the drug entrapment (EE) and loading efficiency (LE).

Cumulative release behaviors of doxorubicin from AgNPs were assessed using acetic acid-triethylamine buffers of different pH. Generally, free Dox or Dox-loaded AgNPs (equivalent to 60 μg of free drug) were sealed in dialysis bags (Cut-off MW: 12,000), which were dropped into brown jars containing 100 mL acid-triethylamine buffer. The jars were then immobilized in a shaking bath which was set at 37 °C, and 180 rpm (IKA® RCT basic, IKA Works GmbH & Co., Germany). At predetermined time point, 3 mL buffer was taken from the jar with equivalent volume of fresh media being added. Dox concentration of the samples were analysed by a fluorospectrophotometry method. To avoid pH induced variations of fluorescence, standard curves of Dox at pH 5.0, 6.0, and 7.4 were separately made to calculate the drug concentration in the release media. The cumulative released drugs were plotted against time to profile the releasing behaviours of AgNP-Dox at different pH. Fluorescence testing set: EX, 490 nm; EM, 590 nm; PMT, 400 V; slit, 5 nm.

A

Drug Loading Potential of dextrin-coated AgNPs							
Dox-SH Concentration (μg/ml)		25	50	100	150	200	250
Entrapment Efficiency (%)		96.5	92.1	90.5	88.6	70.1	58.9
Loading Efficiency (%)	By Dex+Ag	0.048	0.0922	0.181	0.266	0.280	0.295
	By Ag	1.34	2.56	5.03	7.38	7.78	8.18

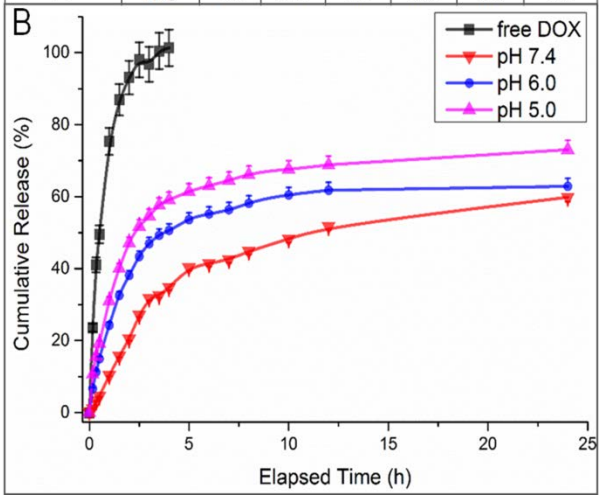

Figure S2 Drug loading potential (A) and pH dependent release profiles (B).

3. Anti-proliferative effects of thiolated Dox and free nanoparticles

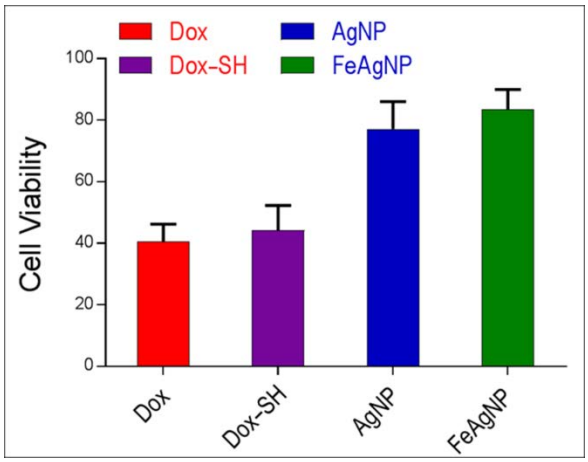

Figure S3 Cell viability of MCF-7 cells treated with 3.4 μmol/L Dox, Dox–SH; or free nanoparticles of equivalent concentrations corresponding to the Dox-loading AgNP-Dox, or FeAgNP-Dox, respectively.

4. Optical imaging of excised and organs from mice treated with free Cy5 dye, or Cy5 labelled nanoparticles.

The optical images of excised s and organs were recorded by the IVIS spectrum imaging system (Perkin-Elmer).

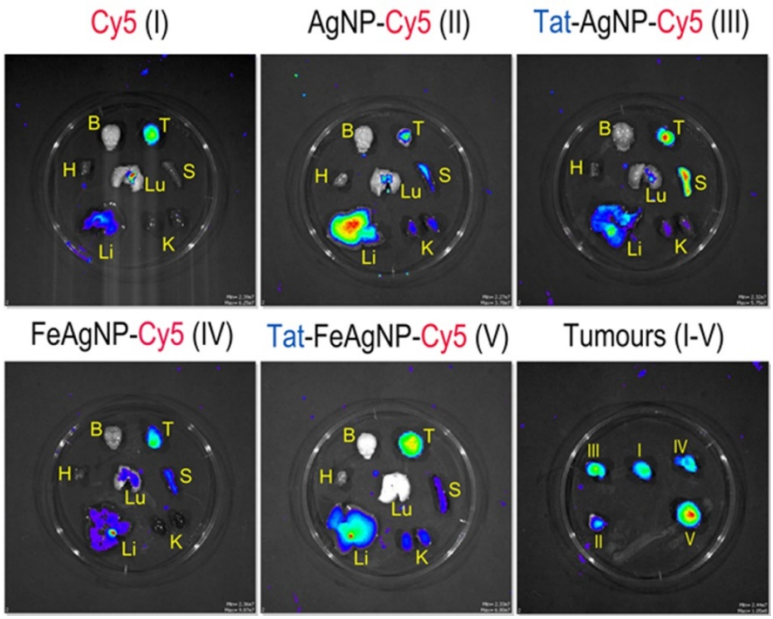

Figure S4 Optical images of excised organs and tumors from mice treated with free Cy5 dye, or Cy5 labelled nanoparticles (Abbreviations: B, brain; T, tumor; H, heart; Lu, lung; S, spleen; Li, liver; K, kidney; and I–V represented Cy5, AgNP-Cy5, Tat-AgNP-Cy5, Fe-AgNP-Cy5, and Tat-FeAgNP-Cy5, respectively.

5. Brain delivery potential of Tat-FeAgNP-Cy5

Brain delivery was assessed on KM mice in a similar procedure as described above: 18 mice were divided into six groups, each was given aforementioned Cy5 or Cy5 labelled nanoparticles. For mice receiving regimentation of FeAgNP-Cy5 and Tat-FeAgNP-Cy5, an external magnet field was applied on the bregma area. Twelve hours later, brain of all mice were excised and be processed into sections (8 μm thick) for microscopic imaging analysis.

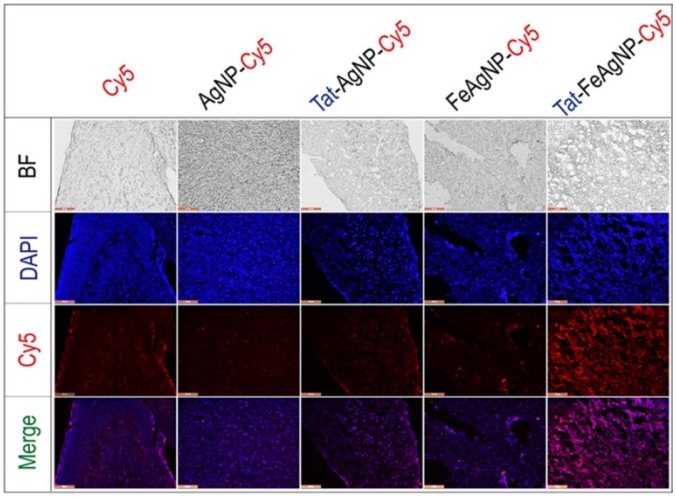

Figure S5 Brain sections of mice receiving different treatment.